Journal of Solid State Chemistry 183 (2010) 890–894

Contents lists available at ScienceDirect

Journal of Solid State Chemistry

journal homepage: www.elsevier.com/locate/jssc

Spin glass transitions in the absence of chemical disorder for the pyrochlores $A_2Sb_2O_7$ (A=Mn, Co, Ni)

H.D. Zhou [a,b], C.R. Wiebe [a,b,*], J.A. Janik [a,b], B. Vogt [b], A. Harter [c], N.S. Dalal [c], J.S. Gardner [d]

[a] Department of Physics, Florida State University, Tallahassee, FL 32306-3016, USA
[b] National High Magnetic Field Laboratory, Florida State University, Tallahassee, FL 32306-4005, USA
[c] Department of Chemistry, Florida State University, Tallahassee, FL 32306-4390, USA
[d] Indiana University, 2401 Milo B. Sampson Lane, Bloomington, IN 47408, USA

ARTICLE INFO

Article history:
Received 19 June 2009
Received in revised form
7 January 2010
Accepted 24 January 2010
Available online 1 February 2010

Keywords:
Geometrically frustrated oxides
Magnetic properties
Pyrochlores
Spin glasses

ABSTRACT

The pyrochlores in the series $A_2Sb_2O_7$ have been synthesized and characterized as exhibiting spin glass transitions at T_{SG}=41, 4.5, and 2.6 K (for A=Mn^{2+} $S=\frac{5}{2}$, Co^{2+} $S=\frac{3}{2}$ and Ni^{2+} S=1, respectively) despite the lack of chemical disorder. Since the Curie–Weiss temperature remains essentially constant for all members in the series ($\theta\sim-40$ K), the frustration index for these materials increases significantly as the moment size is reduced from $f=|\theta|/T_{SG}=1.1$ (Mn^{2+}), to 9.3 (Co^{2+}) to 14.6 (Ni^{2+}). There is also a corresponding change in the spin dynamics measured by the shift in the AC susceptibility signal as a function of frequency. These new materials provide an avenue to investigate the effect of quantum fluctuations on the Heisenberg pyrochlore lattice in the low spin limit, and show there is a dramatic change in the spin dynamics as the quantum regime is approached.

1. Introduction

Geometrically frustrated magnetism has proven to be a fruitful area of study for solid state chemists over the last few decades. Many theorists are still struggling to understand the wide variety of ground state observed in these systems, such as spin glassiness in the absence of chemical disorder, spin ice freezing in systems with large dipolar interactions, and even spin liquid candidates which remain quantum disordered down to zero Kelvin [1,2]. Remarkably, all of these phases have been observed in the cubic pyrochlore lattice $A_2B_2O_7$, a network of corner-shared tetrahedra which has become a model system for the testing of exotic ideas in condensed matter physics. One of the more troubling questions which has arose out of this research is the nature of the spin glass state in systems such as $Y_2Mo_2O_7$, which have little or no bond disorder [3]. Although the freezing of spin fluctuations at T_{SG}=22 K has been demonstrated through neutron scattering measurements, these systems have some properties which deviate from the canonical spin glasses and merit future research to understand the nature of the phase transition [4].

In this paper we report the synthesis and characterization of the pyrochlores in the series $A_2Sb_2O_7$ (A=Mn, Co, Ni), and show that these systems also have glassy transitions at T_{SG}=41, 4.5, and 2.6 K in the apparent absence of bond disorder, much like $Y_2Mo_2O_7$. In these new pyrochlores, the value of the spin can be tuned from $S=\frac{5}{2}$ (Mn^{2+}) to $S=\frac{3}{2}$ (Co^{2+}) to S=1 (Ni^{2+}) with little change in the Weiss temperature $\theta\sim-40$ K. This provides a route to investigating spin dynamics of this glassy state as the quantum regime is approached in the limit of low spin. Surprisingly, the frustration index, as defined by Ramirez as $f=|\theta|/T_{SG}$ increases by an order of magnitude as the moment size decreases from $S=\frac{5}{2}$ to 1 [2]. As well, there is a corresponding change in spin dynamics as measured through the Mydosh parameter for the shift in the AC susceptibility peak at T_{SG} as a function of driving frequency [5].

2. Experimental

Polycrystalline samples of $A_2Sb_2O_7$ (A= Mn, Co, Ni) were prepared through a technique that was outlined by Brisse and refined to give a pure product [6,7]. Mixtures of acetates, $Mn(Ac)_2\cdot 4H_2O$, $Co(Ac)_2\cdot 4H_2O$, $Ni(Ac)_2\cdot 2H_2O$, and antimonic acid ($Sb_2O_5\cdot xH_2O$) in the appropriate stoichiometric ratios were ground and calcined in air at 150 °C for 12 h, then reground and finally calcined in air at 450 °C for 12 h. All samples were single-phase as determined by Powder X-ray diffraction (XRD) with a Cu $K_{\alpha 1}$ source. DC magnetic susceptibility measurements were made with a Quantum Design DC superconducting quantum interference device (SQUID) magnetometer with applied fields of H=0.1 and 1 T. Thermoremanent magnetization (TRM)

* Corresponding author at: Department of Chemistry, University of Winnipeg, Winnipeg, MB, Canada R3B 2E9.
E-mail address: ch.wiebe@uwinnipeg.ca (C.R. Wiebe).

0022-4596/$ - see front matter © 2010 Published by Elsevier Inc.
doi:10.1016/j.jssc.2010.01.025

measurements were also performed on the SQUID. The procedure for TRM relaxation was the following: the samples were field cooled (H=300 Oe) down from 200 K to the measuring temperatures, which are 33, 3 and 2 K for $Mn_2Sb_2O_7$, $Co_2Sb_2O_7$, and $Ni_2Sb_2O_7$, respectively. After the temperature was stabilized we waited for a certain time t_w (between 0 and 2000 s). Thereafter the field was reduced to zero and the magnetization was recorded as a function of the elapsed time. AC magnetization was measured with a physical property measurement system (PPMS).

3. Results

Fig. 1 shows the Rietveld refinement for the $A_2Sb_2O_7$ XRD pattern with Rp ≈ 9, Rwp ≈ 13 and $\chi^2 \approx 3.0$ using the program FullProf. $A_2Sb_2O_7$ (A=Mn, Co, Ni) all have the cubic pyrochlore structure with space group Fd-3m. The lattice parameters are a=10.1664(3) Å, 10.0489(6) Å, and 9.9685(7) Å, for $Mn_2Sb_2O_7$, $Co_2Sb_2O_7$, and $Ni_2Sb_2O_7$, respectively. With decreasing radius of A^{2+}, a decreases (Fig. 2). The eight-fold coordinated magnetic ions, A^{2+}, occupy the corner shared tetrahedral sublattice (inset of Fig. 1(a)). We tested for site disorder by allowing for free refinements on these sites, which to within an error of 1% always refined to full occupancy by one type of ion on each of the

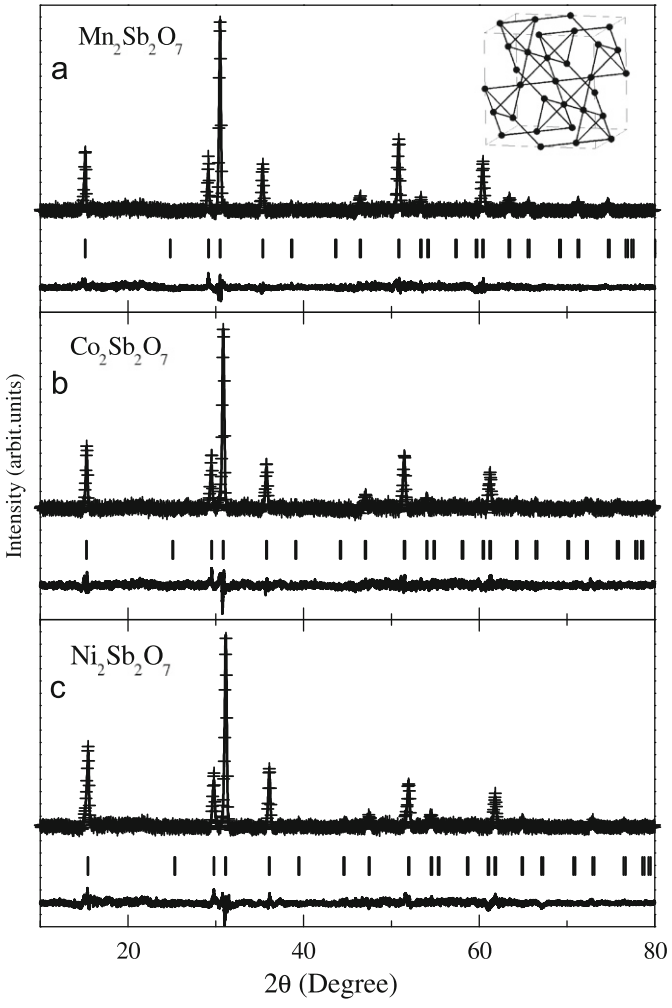

Fig. 1. XRD patterns (plus marks) for $Mn_2Sb_2O_7$ (a), $Co_2Sb_2O_7$ (b), and $Ni_2Sb_2O_7$ (c). The solid curves are the best fits from the Rietveld refinement using FullProf. The vertical marks indicate the position of Bragg peaks, and the bottom curves show the difference between the observed and calculated intensities. The inset of (a) shows a figure of the magnetic A^{2+} ion sublattice.

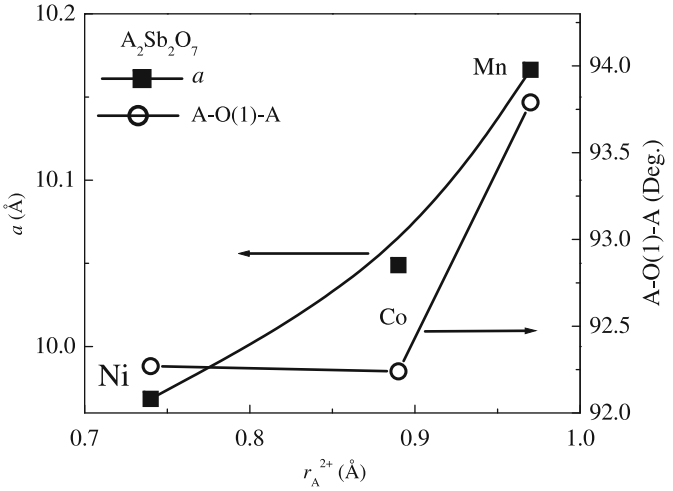

Fig. 2. The variances of lattice parameter and A–O(1)–A angle of $A_2Sb_2O_7$ with the radius of A^{2+}.

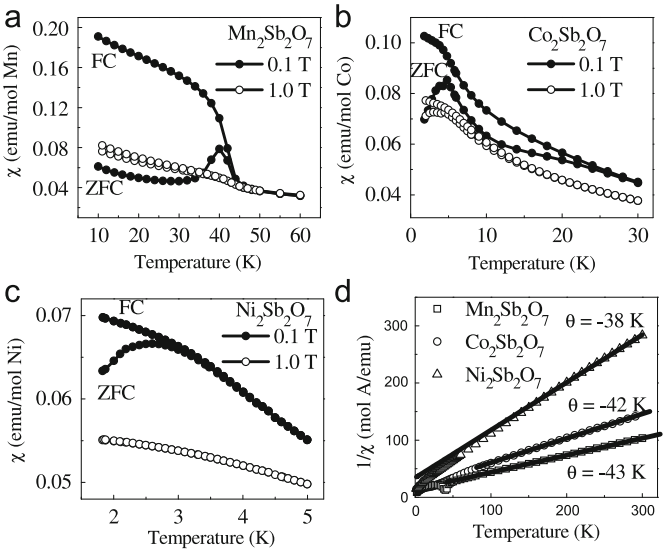

Fig. 3. DC susceptibility showing zero field cooled (ZFC) and field cooled (FC) data at 0.1 and 1 T for (a) $Mn_2Sb_2O_7$, (b) $Co_2Sb_2O_7$, and (c) $Ni_2Sb_2O_7$. (d) Indicates the Curie–Weiss fits to the three compounds, with the associated Weiss temperatures.

A and B sites in $A_2B_2O_7$. There are two reasons for this: (1) the size difference between A^{2+} and Sb^{5+} and (2) the charge difference between the two ions, which suggests that due to electrostatic repulsion, the 5+ ions will order themselves such as to minimize the Coulomb repulsion within the pyrochlore lattice.

Figs. 3(a)–(c) show the temperature dependence of both zero field cooled (ZFC) and field cooled (FC) DC susceptibility measured at H=0.1 and 1 T for $A_2Sb_2O_7$. The ZFC curves at H=0.1 T show a transition at T_{SG}=41, 4.5, and 2.6 K for $Mn_2Sb_2O_7$, $Co_2Sb_2O_7$, and $Ni_2Sb_2O_7$, respectively. Below T_{SG}, there is a divergence between ZFC and FC curves for all three samples, and with higher applied field this divergence is suppressed. This is expected for the weak magnetism associated with canonical spin glasses. For $Co_2Sb_2O_7$, the divergence of ZFC and FC curves starts around 25 K, which is above its T_{SG}. This is typical of spin glasses which have strong exchange interactions and/or short-ranged ordering occuring at higher temperatures. The Curie–Weiss temperature (θ) and effective magnetic moment (μ_{eff}) obtained from linear fits of $1/\chi$ at high temperatures, Fig. 3(d), are −43 K (5.2μ_B), −42 K (3.6μ_B),

and −38 K (2.7μ_B) for $Mn_2Sb_2O_7$, $Co_2Sb_2O_7$, and $Ni_2Sb_2O_7$, respectively. The Curie constants are consistent with the assigned oxidation states of Mn^{2+} ($S=\frac{5}{2}$, $\mu_{eff}=5.9\mu_B$), Co^{2+} ($S=\frac{3}{2}$, $\mu_{eff}=3.9\mu_B$), and Ni^{2+} (S=1, $\mu_{eff}=2.8\mu_B$). For all three samples, the M–H curves (Fig. 4) do not saturate at the highest field of 5 T, which is consistent with the behavior expected of a spin glass. The $Mn_2Sb_2O_7$ sample shows a clear hysteresis loop at low field (Fig. 4(a)), which is much smaller for $Co_2Sb_2O_7$ and $Ni_2Sb_2O_7$ samples (Figs. 4(b) and (c)).

Fig. 5 shows the temperature dependence of the real component of AC magnetization m' for frequency $\omega=1$ and 100 Hz. All the curves show a cusp around T_{SG}. With increasing frequency, the peak shifts to higher temperature and the intensity decreases. The calculated Mydosh parameter, $\Delta T_{SG}/[T_{SG}\log(\omega)]$, for $Mn_2Sb_2O_7$ is 0.0024, which is in the range for canonical spin glasses. For $Co_2Sb_2O_7$ and $Ni_2Sb_2O_7$ the calculated numbers are 0.053 and 0.064, which are slightly larger than the typical value for spin glasses but still one order smaller than the value for superparamagnets [5].

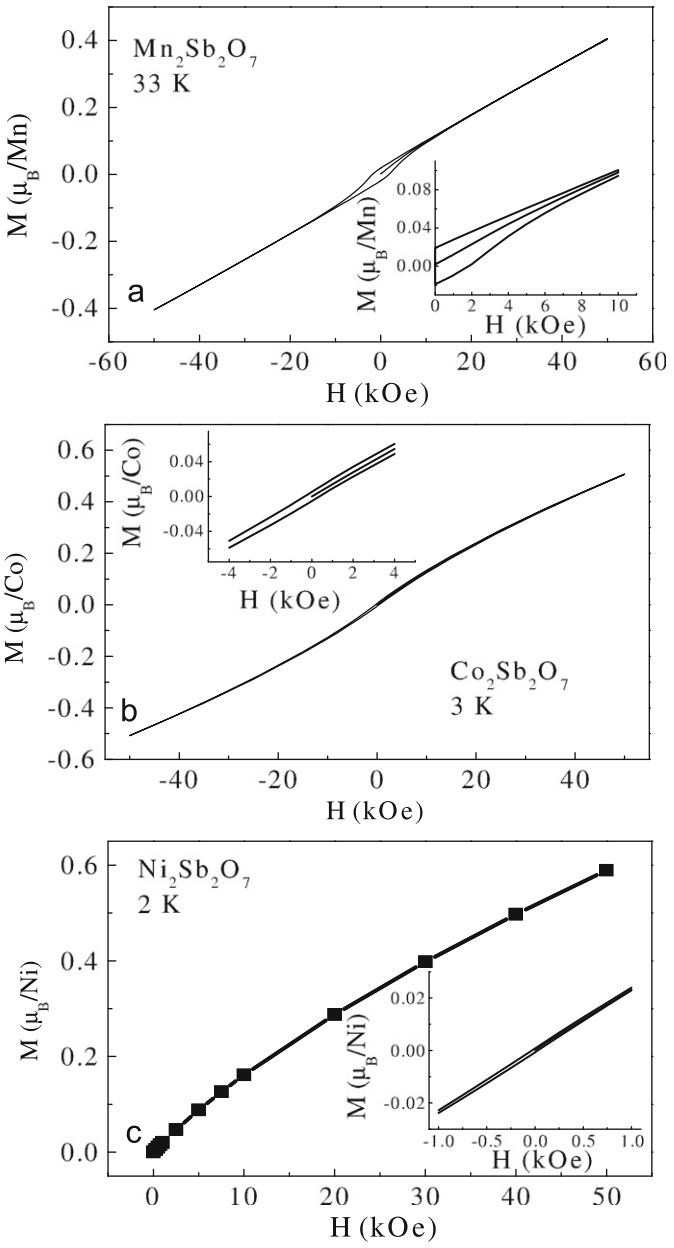

Fig. 4. M–H curves for (a) $Mn_2Sb_2O_7$ at 33 K, (b) $Co_2Sb_2O_7$ at 3 K, and (c) $Ni_2Sb_2O_7$ at 2 K. Insets: Low field portion of the M–H curves.

Although the DC susceptibility of $Mn_2Sb_2O_7$ shows a clear transition at 41 K, the difference between the neutron diffraction measurements at 4 and 80 K shows no new magnetic Bragg peaks. There is no magnetic ordering nor any detectable distortion of the lattice [7]. The nonexistence of magnetic ordering at low temperature, the divergence between ZFC and FC curves, and the cusp of the AC magnetization are all consistent with a spin glass transition at T_{SG} for $A_2Sb_2O_7$ (Table 1).

In order to further check the existence of spin-glass behavior, TRM measurements were performed, shown in Fig. 6. For all three samples, a temperature below their T_{SG} is selected for the TRM measurements. The temperatures are 33, 3 and 2 K for $Mn_2Sb_2O_7$, $Co_2Sb_2O_7$, and $Ni_2Sb_2O_7$, respectively. The results of the three samples clearly show the magnetization relaxation. All of the curves can be described by the stretched exponential model,

$$M(t)=M_0+M_r\exp[-(t/t_p)^{1-n}] \quad (1)$$

here M_0 relates to a magnetic component and M_r to a glassy component mainly contributing to the relaxation observed effects. Both M_r and t_p (the time constant) depends on temperature (T) and t_w, while n is only a function of T. If n=0, there is a single time-constant, exponential relaxation; and if n=1, there is no relaxation at all. The solid curves in Figs. 6(a–c) are the best fits of Eq. (1) to the experimental data, with parameters listed in Table 2. The changes observed in $M(t)$ measured for different values of t_w demonstrate the occurrence of aging effects. In the inset of Figs. 6(a–c) this point is emphasized by showing the relaxation rate $S(t)=dM/d\ln(t)$. The shift of the minimum position of $S(t)$ is clearly observed, which is expected to occur for a spin glass system [8].

4. Discussion

The neutron diffraction measurements show that there is no magnetic ordering nor any detectable distortion of the lattice for $Mn_2Sb_2O_7$ below T_{SG} [7]. The spin glass transition in $Mn_2Sb_2O_7$ without apparent chemical disorder and structural distortion is reminiscent of other frustrated systems that show glassy behavior such as $Y_2Mo_2O_7$ [9] or Sr_2MgReO_6 [10]. The glassiness of the system implies some kind of disorder in the exchange integral, whose origin might be a deformation at the local ionic environment. Indeed, the X-ray absorption fine structure (XAFS) measurements have shown that the Mo tetrahedra of $Y_2Mo_2O_7$ are in fact distorted at the local level by 5% [11]. This amount of bond disorder is not seen by the usual diffraction techniques (X rays or neutrons), indicating that the average bulk structure is almost the perfect oxide pyrochlore lattice. Here the glassiness of $Mn_2Sb_2O_7$ could have a similar origin—the local deformed lattice.

The frustration factor, as introduced by Ramirez to describe geometrically frustrated magnets (GFM), changes as a function of spin in these pyrochlores from $f\sim\theta/T_{SG}\sim1.1$ (Mn) to 9.3 (Co) to 14.6 (Ni), over an order of magnitude across the series (Fig. 7). Strongly frustrated systems have been assigned the arbitrary criterion $f\geq10$, so in this case the Co and Ni pyrochlores fall within this regime [2]. By comparison, other geometrically frustrated systems which show glassiness have values of $f\sim10$ for $Y_2Mo_2O_7$, and in two dimensions, this number tends to be much larger, such as $f\sim51$ for the kagome jarosite $(D_3O)Fe(SO_4)_2(OD)_6$ [1]. The physical mechanism for glassiness in 2D may be fundamentally different for 3D, however, since in 2D there could be a Kousterlitz–Thouless like transition where for 3D there is no predicted spin glass state, even with single ion anisotropy [12].

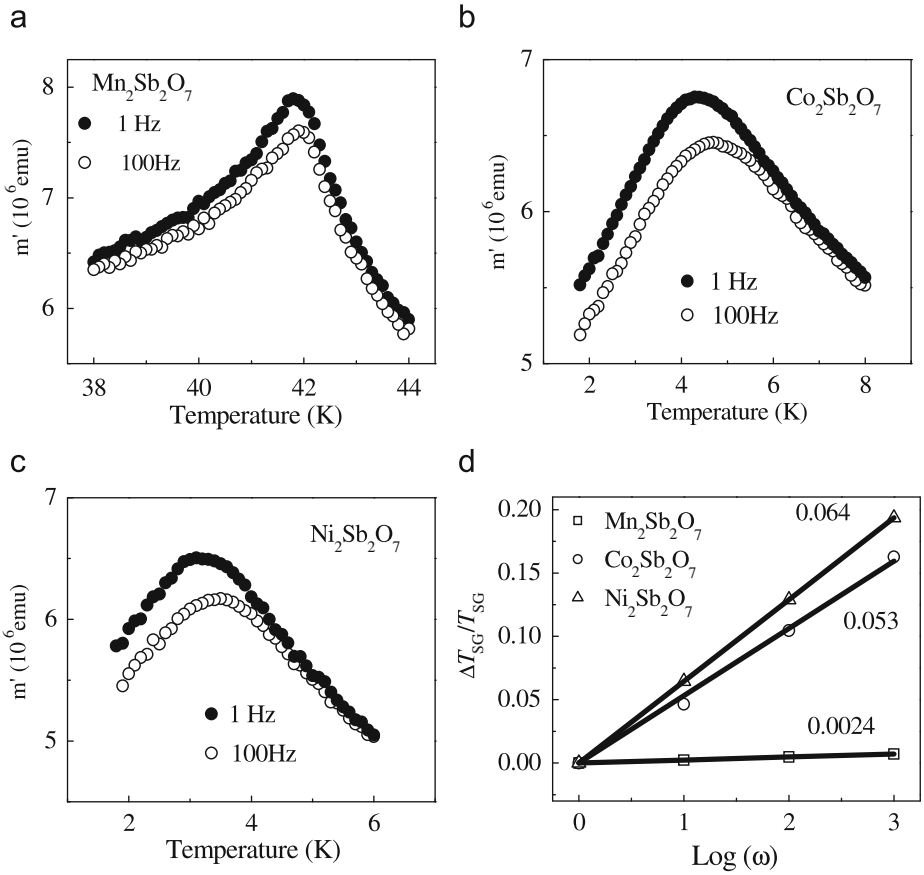

Fig. 5. The real part of the AC magnetization of (a) $Mn_2Sb_2O_7$, (b) $Co_2Sb_2O_7$, and (c) $Ni_2Sb_2O_7$ as a function of frequency shows a shift at T_{SG}. (d) $\Delta T_{SG}/T_{SG}$ is plotted as a function of the frequency.

Table 1
Crystallographic parameters and selected bond lengths and angles for $A_2Sb_2O_7$.

Sample	Atom	x	y	z	B (Å^2)
$Mn_2Sb_2O_7$	Mn	0.5	0.5	0.5	1.57(1)
	Sb	0	0	0	0.80(4)
	O(1)	0.3345(16)	0.125	0.125	2.60(2)
	O(2)	0.375	0.375	0.375	2.01(2)
	a	10.1664(3)(Å)			
	Mn–O(1)	2.46(2)(Å)			
	Mn–O(2)	2.20(1)(Å)			
	Mn–O(1)–Mn	93.79(4)°			
	Mn–O(2)–Mn	109.47(1)°			
$Co_2Sb_2O_7$	Co	0.5	0.5	0.5	1.77(4)
	Sb	0	0	0	0.87(5)
	O(1)	0.3299(20)	0.125	0.125	2.75(2)
	O(2)	0.375	0.375	0.375	2.32(3)
	a	10.0489(6)(Å)			
	Co–O(1)	2.46(4)(Å)			
	Co–O(2)	2.17(5)(Å)			
	Co–O(1)–Co	92.24(3)°			
	Co–O(2)–Co	109.47(1)°			
$Ni_2Sb_2O_7$	Co	0.5	0.5	0.5	1.87(4)
	Sb	0	0	0	0.90(3)
	O(1)	0.3301(25)	0.125	0.125	2.85(4)
	O(2)	0.375	0.375	0.375	2.22(2)
	a	9.9685(7)(Å)			
	Ni–O(1)	2.44(4)(Å)			
	Ni–O(2)	2.15(8)(Å)			
	Ni–O(1)–Ni	92.27(5)°			
	Ni–O(2)–Ni	109.47(1)°			

The relative lack of change in the Curie–Weiss temperature is unusual and implies that the interaction energy J changes as a function of spin (in the absence of significant changes in bond distance or orbital overlap). From mean field theory, the Curie–Weiss temperature is related to J through:

$$\theta = [2S(S+1)/3k]\sum z_n J_n \quad (2)$$

where S is the spin, n is the nearest neighbor index and J_n the exchange constant [1]. Therefore, if θ is constant but the magnitude of the spin is changing, then this implies that the interactions between the spins, J, are also changing. Using this simple model, one can calculate the ratio of the sum of the exchange constants from the Mn pyrochlore compared to the Ni to be $(S+1)S/S'(S'+1) \sim \Sigma z_n J_n / \Sigma z'_n J'_n \sim 6$, indicating almost an order of magnitude enhanced exchange.

What is the mechanism for the enhanced exchange? It is difficult to attribute the change in J due to a change in the electronic orbital overlap alone. The A–O–A bond angle change due to the decrease of the lattice constant from the Mn to the Ni sample, for example, is only 4% (Fig. 2). It is well-known that many highly correlated electron systems, such as CuO (the parent compound of high-T_C superconductors), have superexchange interactions J which are highly dependent upon the bond angle [13,14]. However, even in these cases, a change of only 4% of the A–O–A bond angle cannot account for nearly an order of magnitude change in J. Furthermore, there is a systematic change in the spin dynamics as the magnitude of the moment is lowered across the series. Given this information, it seems that the enhancement of quantum fluctuations (by reducing the magnitude of the spin upon the A-sites) has a direct effect upon

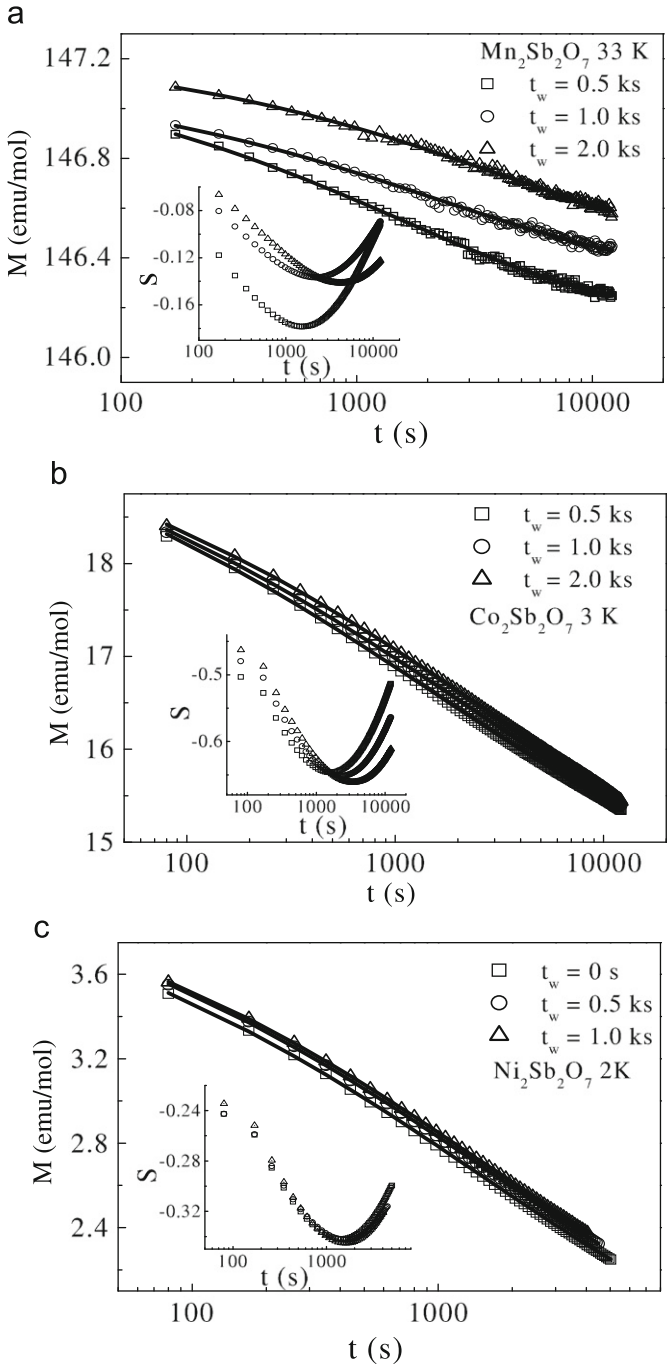

Fig. 6. TRM measurements on (a) $Mn_2Sb_2O_7$, (b) $Co_2Sb_2O_7$, and (c) $Ni_2Sb_2O_7$.

the dynamics of these systems, leading to a higher frustration index and faster spin dynamics.

Among the studied pyrochlores, there are few examples in the literature of magnetic transition metal ions found upon A-sites that can be systematically tuned such as the case of $A_2Sb_2O_7$. In fact, most known studies have been completed on rare-earth pyrochlores where crystal field effects tend to dictate the relevant energy scales and interactions [1]. The stabilization of the pyrochlore structure using an antimony sublattice provides a new avenue towards exploring quantum magnetism through

Table 2
Parameters used to fit the TRM data with Eq. (1) for $A_2Sb_2O_7$.

$A_2Sb_2O_7$	T (K)	t_w (s)	M_0 (emu/mol)	M_r (emu/mol)	t_p (s)	n
Mn	33	500	146.4(6)	0.80(1)	2200(10)	0.50(1)
		1000		0.79(1)	3000(12)	
		2000		0.78(1)	4220(10)	
Co	3	500	14.2(2)	6.10(1)	1626(6)	0.30(1)
		1000		5.92(2)	2232(10)	
		2000		5.87(1)	3372(12)	
Ni	2	0	1.76(2)	2.43(2)	1420(10)	0.38(2)
		500		2.41(1)	1550(10)	
		1000		2.38(2)	1600(10)	

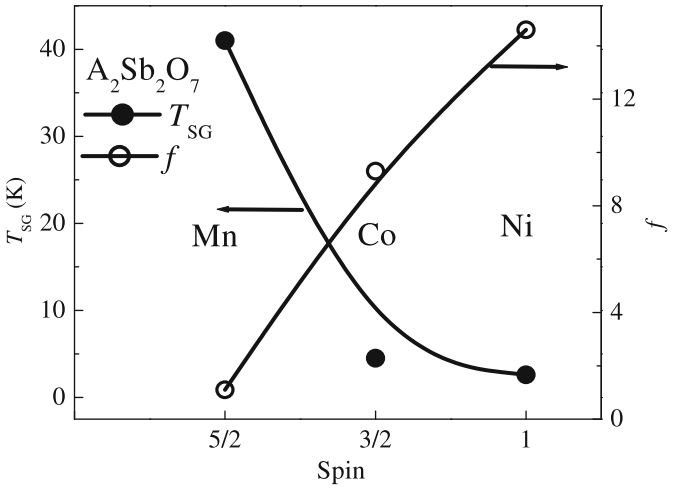

Fig. 7. The plots of T_{SG} and f as a function of the spin of A^{2+} for $A_2Sb_2O_7$.

doping in the limit of low spin. Future studies are underway to find $S=\frac{1}{2}$ candidates that may display unusual ground states, and to further explore the spin dynamics within these new systems using relevant probes (NMR, muon spin relaxation, and high-resolution inelastic neutron scattering experiments) [10].

Acknowledgments

This work utilized facilities supported in part by the NSF Grant DMR-0504769. A portion of this work was made possible by the NHMFL IHRP, the EIEG Program, and the State of Florida.

References

[1] J.E. Greedan, J. Mater. Chem. 11 (2001) 37–53.
[2] A.P. Ramirez, Ann. Rev. Mater. Sci. 24 (1994) 453.
[3] J.S. Gardner, et al., Phys. Rev. Lett. 83 (1999) 211.
[4] J.E. Greedan, et al., Solid State Commun. 59 (1986) 895.
[5] J. Mydosh, Spin Glasses: An Experimental Introduction, Taylor & Francis, London, 1995.
[6] O. Knop, F. Brisse, Am. Chem. Soc. Bull. 46 (1967) 881.
[7] H.D. Zhou, et al., J. Phys. Condens. Matter 20 (2008) 325201.
[8] See for example K. Binder, A.P. Young, Rev. Mod. Phys. 58 (1986) 801.
[9] J.N. Reimers, et al., J. Solid State Chem. 72 (1988) 390.
[10] C.R. Wiebe, et al., Phys. Rev. B 68 (2003) 134410.
[11] C.H. Booth, et al., Phys. Rev. B 62 (2000) R755.
[12] J.M. Kosterlitz, D.J. Thouless, J. Phys. C 6 (1973) 1181.
[13] T. Shimazu, T. Matsumoto, T. Goto, K. Yoshimura, K. Kosuge, J. Phys. Soc. Japan 72 (2003) 2165.
[14] T. Kimura, et al., Nat. Mater. 7 (2008) 291.